



Titre: Fluidic patch antenna based on liquid metal alloy/single-wall
Title: carbon-nanotubes operating at the S-band frequency

Auteurs: Brahim Aïssa, Mourad Nedil, M. A. Habib, E. Haddad, Wes Jamroz,
Authors: Daniel Therriault, Y. Coulibaly, & Federico Rosei

Date: 2013

Type: Article de revue / Article

Référence: Aïssa, B., Nedil, M., Habib, M. A., Haddad, E., Jamroz, W., Therriault, D., Coulibaly,
Citation: Y., & Rosei, F. (2013). Fluidic patch antenna based on liquid metal alloy/single-wall
carbon-nanotubes operating at the S-band frequency. Applied Physics Letters,
103(6), 063101 (5 pages). <https://doi.org/10.1063/1.4817861>

 **Document en libre accès dans PolyPublie**
Open Access document in PolyPublie

URL de PolyPublie: <https://publications.polymtl.ca/10402/>
PolyPublie URL:

Version: Version officielle de l'éditeur / Published version
Révisé par les pairs / Refereed

Conditions d'utilisation: Tous droits réservés / All rights reserved
Terms of Use:

 **Document publié chez l'éditeur officiel**
Document issued by the official publisher

Titre de la revue: Applied Physics Letters (vol. 103, no. 6)
Journal Title:

Maison d'édition: AIP
Publisher:

URL officiel: <https://doi.org/10.1063/1.4817861>
Official URL:

Mention légale: ©2013. This is the author's version of an article that appeared in Applied Physics
Letters (vol. 103, no. 6) . The final published version is available at
Legal notice: <https://doi.org/10.1063/1.4817861>

% & ' () * * " + & ! & ' " # \$ # , - - & ! &



View Online



Export Citation



CrossMark

! " # \$ % & ' () * ' + & # , " & ! & " & - # ,

* - . ! & ' / & (- -- 0 - ' * * (* * - *
+ & - . * . 1 " 1 2 ! " 1 1 2

/ & (* ' & - ' - * - -- ! " #
* / 0 " " 1 !

. / & - * . - ! / & (- -- 3 & - 0 -
* // 2 ! 1

 QBLOX



1 qubit

Shorten Setup Time

Auto-Calibration

More Qubits

Fully-integrated

Quantum Control Stacks

Ultrastable DC to 18.5 GHz

Synchronized <<1 ns

Ultralow noise



100s qubits

[visit our website >](#)

Fluidic patch antenna based on liquid metal alloy/single-wall carbon-nanotubes operating at the S-band frequency

B. Aïssa,^{1,2,3,a)} M. Nedil,⁴ M. A. Habib,⁵ E. Haddad,¹ W. Jamroz,¹ D. Therriault,² Y. Coulibaly,⁴ and F. Rosei³

¹Department of Smart Materials and Sensors for Space Missions, MPB Technologies, Inc., 151 Hymus Boulevard, Montreal H9R 1E9, Canada

²Center for Applied Research on Polymers (CREPEC), Mechanical Engineering Department, Ecole Polytechnique de Montreal, P.O. Box 6079, Montreal H3C 3A7, Canada

³Centre Energie, Matériaux et Télécommunications, INRS, 1650, Boulevard Lionel-Boulet Varennes, Quebec J3X 1S2, Canada

⁴Laboratoire de Recherche Québec en Communications Souterraines, UQAT, 450, 3e Avenue, Val-d'Or J9P 1S2, Canada

⁵Department of Computer Science, Yanbu University College, P.O. Box 30031, Kingdom of Saudi Arabia

(Received 26 April 2013; accepted 24 July 2013; published online 6 August 2013)

This letter describes the fabrication and characterization of a fluidic patch antenna operating at the S-band frequency (4 GHz). The antenna prototype is composed of a nanocomposite material made by a liquid metal alloy (eutectic gallium indium) blended with single-wall carbon-nanotube (SWNTs). The nanocomposite is then enclosed in a polymeric substrate by employing the UV-assisted direct-writing technology. The fluidic antennas specimens feature excellent performances in perfect agreement with simulations, showing an increase in the electrical conductivity and reflection coefficient with respect to the SWNTs concentration. The effect of the SWNTs on the long-term stability of antenna's mechanical properties is also demonstrated. © 2013 AIP Publishing LLC
[\[http://dx.doi.org/10.1063/1.4817851\]](http://dx.doi.org/10.1063/1.4817851)

The past decade has witnessed the rapid growth of communication and sensing applications, leading to an escalating demand for advances in antenna technologies, including flexible mobile communications, compact high gain patch antenna, or the multiple-input multiple-output (MIMO) channel technologies.⁶ Although copper and other solid conductors can provide highly efficient antennas, the fatigue of copper eventually deformed for general adaptive antenna applications (such as the co-planar, sheet-like geometry of a patch or Flexible antennas have the potential to enhance the emerging field of flexible electronics.^{7,8} Bendable antennas are also of interest for smart antenna applications such as beamforming and beam-bending antennas for limited and nonplanar spaces,¹⁰ and antennas for wearable health-monitoring devices, aeronautic remote sensing, or wireless strain sensors using printed radio frequency identification (RFID) tags.^{3,11,13}

Fluidic-method has additional advantages: (i) The process is fairly simple and scalable and can be adopted to other flexible 2D and 3D devices; (ii) it allows the antenna to be integrated with other fluidic components for tuning, sensing, and signal modulation, (iii) it does not involve etching or plating and thus does not produce hazardous waste. There are, however, challenges associated with shaping the fluid metal into more complex geometries that go beyond simple dipoles (such as the co-planar, sheet-like geometry of a patch or flexible antenna) due to non-uniform filling of wide microchannels. In addition, using metal liquid alone within a flexible host polymer has shown very often a poor mechanical durability.^{14,15}

In this letter we report on the incorporation of single-walled carbon nanotubes (SWNTs) within a EGaln metal liquid alloy, yielding the fabrication of a fluidic flexible patch antenna operating at 4 GHz (S-band), thereby obtaining a radiating antenna-structure element with improved electrical properties and stable mechanical durability. Based on our simulations results, we used our developed UV-assisted direct-writing technology to design the patch antenna onto a Galinstan, Ga 68.5%, In 21.5%, and Sn 10% PDMS substrate, followed by injecting and encapsulating the conductive EGaln/SWNT nanocomposites with varying SWNTs loads that serve as a radiant antenna element material. The fluidic antennas specimen exhibited excellent performance in total agreement with our simulations. The room temperature electrical conductivities of these antenna devices were shown to increase with respect to SWNT concentration in the nanocomposite and were about 2 orders of magnitude higher than that of the pure EGaln, when SWNT loads range from 0.5 to 5 wt. % only. More importantly, the associated reflection coefficient has increased up to 10 dB

On the other hand, Kim et al.^{25,26} recently described stretchable integrated circuits with elongation of up to 100% using wavy, thin silicon ribbons on elastic substrates. Besides its ability to produce flexible antennas, this method provides a simple and scalable way to fabricate antennas. In this letter we report on the incorporation of single-walled carbon nanotubes (SWNTs) within a EGaln metal liquid alloy, yielding the fabrication of a fluidic flexible patch antenna operating at 4 GHz (S-band), thereby obtaining a radiating antenna-structure element with improved electrical properties and stable mechanical durability. Based on our simulations results, we used our developed UV-assisted direct-writing technology to design the patch antenna onto a Galinstan, Ga 68.5%, In 21.5%, and Sn 10% PDMS substrate, followed by injecting and encapsulating the conductive EGaln/SWNT nanocomposites with varying SWNTs loads that serve as a radiant antenna element material. The fluidic antennas specimen exhibited excellent performance in total agreement with our simulations. The room temperature electrical conductivities of these antenna devices were shown to increase with respect to SWNT concentration in the nanocomposite and were about 2 orders of magnitude higher than that of the pure EGaln, when SWNT loads range from 0.5 to 5 wt. % only. More importantly, the associated reflection coefficient has increased up to 10 dB

^{a)}Author to whom correspondence should be addressed. Electronic addresses: aissab@emt.inrs.ca and brahim.aissa@mpbc.ca

for the same SWNT variation-range. Finally, the effect of (CP750, Cole Parmer) for 30 min. Figure 1(b) depicts the the SWNTs on the long-term stability of the mechanical simulated geometry and dimensions of the radiating micro-bending is also demonstrated over more than 12 months strip patch antenna operating at 4 GHz S-band frequency which is a fundamental achievement towards realizing (MATLAB[®] solution and CST Microwave Studio[®] 2011 soft-operating-stable bendable antenna devices based on SWNTs were used for parameters calculations). The simulated and metal alloy nanocomposites.

Single wall carbon nanotubes were synthesized by using UV-assisted direct writing technology^{30,32} was then the developed plasma torch technology (detailed process caused to design the patch antenna onto a 500 µm thick PDMS be found in Ref. 27). This process exclusively produces substrate. The fabrication of the radiant antenna structure SWNTs that take growth in the gas-phase. The as-grown began with the deposition of an epoxy/SWNT nanocompo-soot like SWNTs were subsequently purified by an acidic site placement,^{30,33} under continuous UV exposure³⁰ leading treatment through refluxing in a 3M-HNO₃ (Sigma Aldrich) to a solid 2-D antenna pattern (Fig. 1(c)). The shape designed by the nanocomposite placements was then filled with the

The SWNTs were characterized by bright field transmis- EGaIn/SWNTs nanocomposite. The final specimen was then sion electron microscopy (TEM) using a Jeol JEM-2100 F sealed to protect the liquid nanocomposite inside the sample; FEG-TEM (200 kV) microscope. Figure 1(a) shows a repre- a 250 µm of PDMS was gently spin-coated to encapsulate sentative TEM micrograph of the purified SWNT deposit, the fluidic radiant element, followed by a curing step at where bundles of a few SWNTs are containing individual 85 C for 1 h. A V-type feed connector was appropriately tube diameters of about 1.2 nm. These bundles have diam- incorporated to measure antenna performances. Figure 1(e) eters in the 2D 10 nm range and lengths of the order of few shows an optical top-view image of the infiltrated patch leading thereby to SWNT having an aspect ratio over three antenna prototype.

orders of magnitudes. Purified SWNTs were first ultrasoni- Figure 2(a) shows the relationship between the experi- cated in dimethylformamide (1 mg/ml) solution for 5 h to mentally measured electrical conductivity (of the elabo- dissolve bundles, followed by centrifugation at 12 000 rpm rated EGaIn/SWNT nanocomposites with respect to their for 15 min to select well-dispersed, narrow bundles of the nanotube contents (using a Hewlett-Packard 4140B semicon- SWNTs. The centrifuged solution was then held at 60 for ductor parameter analyzer). With an increase of SWNT con- solvent evaporation. This purification process is known to dent, the conductivity gradually increases and is about 2 graft COOH carboxylic acid groups on the nanotube, an in- orders of magnitude higher than that of pure EGaIn, when herent consequence to the chemical process, which favours SWNT loads reach 5 wt. % only. The stepwise change in their dispersion.^{28,29} Appropriate weights of purified SWNT the conductivity of the composites is a direct result of the were then dispersed inside a room temperature liquid EGaIn gradual formation of an interconnected network of SWNT (Sigma Aldrich) using a wand-type ultrasonic processor inside the nanocomposite. Figure 2(b) shows the re-

reflection coefficient S_{11} , as a function of the frequency, for both simu- lation and experiment scenarios (using an Agilent 8722ES network analyzer). The experimental results show that S_{11} increases from $|20|$ dB for a pure EGaIn alloy to reach its highest value of $|30|$ dB for a SWNT load of 5 wt. %, mean- ing that 99% and 99.9% of the input power is radiated from antenna, respectively. Since the pure PDMS polymer is transparent to EM radiation, the measured re- flection coefficient is definitely due to the presence of the conductive material (EGaIn and SWNT). Table I summarizes the main performance parameters of the simulated and fabricated fluidic antennas as a function of the SWNTs concentration inside the nanocomposite. The average experimental uncer- tainty was found about 5% over tens measured prototypes.

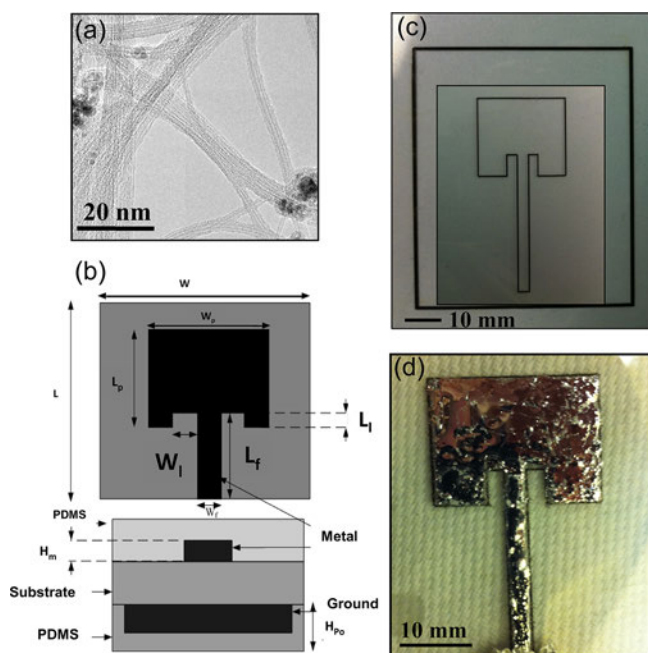


FIG. 1. (a) Representative TEM images of purified SWNTs. (b) Simulated geometry and dimensions of the radiating microstrip patch antenna operating at 4 GHz S-band frequency. (c) Optical top-view image of the epoxy/SWNT-based placements deposited by UV-assisted direct writing technology on a PDMS substrate. (d) Optical top-view image of the infiltrated patch antenna element prototype.

TABLE I. Simulated parameters of the radiating microstrip patch antenna operating at 4 GHz S-band frequency.

Parameters	Values	Parameters	Values
H_m (mm)	0.1	L_p (mm)	22.8
$H_{po} \frac{1}{4} h_{sub}$ (mm)	1	W_f (mm)	2.78
W (mm)	80	L_f (mm)	6.5
L (mm)	80	$\epsilon_{po} \frac{1}{4} \epsilon_{sub}$	2.5
W_f (mm)	2.78	Γ_{EGaIn} (S/cm)	$3.4 \cdot 10^4$
L_f (mm)	40	Γ_{SWNT} (S/cm)	$8.5 \cdot 10^5$
W_p (mm)	24		

FIG. 2. (a) Relationship between the experimentally measured electrical conductivity σ_{dc} of the EGaIn/SWNT nanocomposite with respect to the nanotubes loads. (b) Reflection coefficient S_{11} , as a function of the frequency. (c) Corresponding simulated and experiment radiation patterns (H and E plans) at 4 GHz frequency.

The radiation patterns of the antenna prototype were measured inside an anechoic chamber with a Hybrid Near-Field Antenna Measurement System (HNFAMS) from Antcom Corp. Simulated and measured antenna radiation patterns in the E-plane and the H-plane are shown in Figure 2(c). The fabricated antenna exhibits somehow an omnidirectional broad beam coverage. In fact, the radiation pattern as expected, has a main lobe for the radiation of the patch antenna below the ground plane confirms that the patch antenna does not radiate strongly in this direction. As seen in this figure, good agreement between simulated and measured results was obtained. In addition, it can be noted that the radiation pattern compared to the conventional patch antenna.

The fabricated antenna prototypes were systematically bent inside a tube of particular curvature radius. Figure 3(a) shows the variation of the reflection coefficient as a function of the curvature radius for the simulated antenna and for the

specimen fabricated with SWNT loads of 0 and 5 wt.%, respectively. When the bending angle of the antenna increases, the reflection coefficient decreases accordingly, and is even below the accepted value of $|S_{11}| < -10$ dB for a curvature radius of 5 mm (recorded for the case of a pure EGaIn based prototype). At 30 mm curvature radius, all the antennas recover their initial radiation power (i.e., as that recorded before the bending). It is worth noting here that under the bending process, comparatively to the antenna specimen based on pure EGaIn (i.e., 0 wt. % of SWNT), the incorporation of 5 wt. % of nanotubes within the nanocomposite leads to a considerable improvement of the associated reflection coefficients. This is ascribed to the enhancement of the global mechanical elasticity of the antennas brought by incorporating SWNT inside the nanocomposite. Figure 3(b) illustrates the change in the resonance frequency of the various antennas under different values of curvature. As expected, since the resonant frequency is rather related to the length of the radiant element and the effective dielectric constant of the medium, no significant change is noticed, and the antenna specimens keep a stable radiation frequency within the experimental uncertainties.

Finally, we investigated the reliability of the antenna by repeatedly bent as a function of time. Table III summarizes the long-term performances of the antennas specimen (for two different SWNT loads, namely, 0 and 2 wt. %, respectively). Even after being bent over 100 times (12 months after the first measurement under ambient conditions), the antenna specimen containing 2 wt. % only of nanotube exhibited a return losses nearly the same (within 4.3%

TABLE II. Main antenna performance parameters (simulation and experiment) with respect to the nanotube contents into the nanocomposite.

CNT load (wt. %)	Simulations	0	0.5	1	2	3	5
Res. freq. (GHz)	4	4.03	4.02	4.01	4.01	4.02	4.02
$ S_{11} $ (dB)	43	20	22	23	23	24	30
$ FWHM _{GHz}$	0.2	2.16	2.08	2	1.7	1.5	1.2

FIG. 3. (a) Return losses (reflection coefficient) at 4 GHz and (b) the resonance frequency for the simulated antenna, and these fabricated with SWNT loads of 0 and 5 wt. %, as a function of the curvature radius in mm.

fluctuation) as that of the initial measurement (the effect of SWNTs on antenna performance is in progress). On the contrary, the specimen with 5 wt. % SWNT content manifests a fluctuation up to 13%. No changes were noticed for the resonance frequency parameter, which remains stable in both cases (with and without SWNT). Thus, the combination of a liquid metal antenna concept is promising for fluidic antennas that can be used in wireless sensing or monitoring radio systems, switches, RFID tags, conformal circuits for health monitoring, or in military and space applications. Repeatedly returns to its original shape, even after multiple deformations, without losing its electromagnetic properties.

We note that the tendency revealed by Fig. 3(b) closely suggests a possible direct correlation between the S_{11} of the antenna specimens and their electrical conductivity (and hence with the SWNTs-concentrations within

FIG. 4. Reflection coefficient (S_{11}) at 4 GHz for the whole fabricated prototypes as a function of their associated electrical conductivities and SWNT loads.

the nanocomposite). By cross-plotting the S_{11} at 4 GHz of all the fabricated prototypes as a function of their associated r_{dc} values, Figure 4 confirms that the antenna performances of all the investigated samples increase proportionally with respect to their electrical conductivity.³⁴ However, despite this experimental evidence, advanced characterizations and studies are required to determine the exact influence of the other involved factors, such as radiant-element thickness, and the effect of other frequency domains.

In summary, by using the UV assisted direct-writing technology, we demonstrated the fabrication of a fluid patch antenna based on a conductive nanocomposite material that consists of a liquid metal alloy (EGaIn) blended with SWNTs. The antennas prototypes, operating at the S-band frequency domain, have shown radiation characteristics of 90% efficiency and above (i.e., $|S_{11}| < 10$ dB). These antennas have displayed a resonant frequency and return losses (S_{11}) that are function of the SWNTs concentrations, in a good agreement with simulations modeling. The presented concept is promising for fluidic antennas that can be used in wireless sensing or monitoring radio systems, switches, RFID tags, conformal circuits for health monitoring, or in military and space applications.

We acknowledge financial support from the Canada Foundation for Innovation, the Natural Science and Engineering Research Council (NSERC) of Canada, the Fonds Québécois de la Recherche sur la Nature et les Technologies (FQRNT). F.R. is grateful to the Canada

TABLE III. Long-term antenna returns losses over storage under ambient conditions.

	Day 1	Month 1	Month 4	Month 7	Month 10	Month 12	Fluct.%
$ S_{11} $ (dB) - 0 wt. % CNT	20	20	19	18.5	18	17	13%
$ S_{11} $ (dB) - 2 wt. % CNT	23	23	23	23	22.5	22	4.3%

- Research Chairs Program for partial salary support. B.A. is grateful to F. Larouche (Raymor Ind.) for supplying the SWNTs.
- ¹S. H. Kim, C. Jang, K. J. Kim, S. Ahn, and K. C. Choi, *IEEE Trans. Electron Devices* **57**, 3370 (2010).
 - ²J.-K. Lee, Y.-S. Lim, C.-H. Park, Y.-I. Park, C.-D. Kim, and Y.-K. Hwang, *IEEE Electron Device Lett* **31**, 833 (2010).
 - ³S. Merilampi, T. Børninen, L. Ukkonen, P. Ruuskanen, and L. Sydänheimo, *Sens. Rev* **31**, 32 (2011).
 - ⁴Y. K. Bekali and M. Essaaidi, *Microwave Opt. Technol. Lett* **55**, 1622 (2013).
 - ⁵J. H. Wang, L. Sang, Z. G. Wang, R. M. Xu, and B. Yan, *Electromagn. Waves Appl* **27**, 330 (2013).
 - ⁶E. Björnson, P. Zetterberg, M. Bengtsson, and B. Otterstedt, *IEEE Commun. Lett* **17**, 91 (2013).
 - ⁷J. T. Bernhard, in *Reconfigurable Antennas, Encyclopedia of RF and Microwave Engineering*, edited by K. Chang (Wiley, New York, 2005).
 - ⁸J.-C. Langer, C. Liu, and J. T. Bernhard, *IEEE Microw. Wirel. Compon. Lett* **13**, 120 (2003).
 - ⁹P. S. Hall and S. J. Vetterlein, *IEEE Proc.* **137**(5), 293 (1990).
 - ¹⁰N. Tiercelin, P. Coquet, R. Sauleau, V. Senez, and H. Fujita, *J. Micromech. Microeng* **16**, 2389 (2006).
 - ¹¹V. Lumelsky, M. Shur, and S. Wagner, *IEEE Sens. J* **1**, 41 (2001).
 - ¹²R. H. Reuss, B. R. Chalamala, A. Moussessian, M. G. Kane, A. Kumar, D. C. Zhang, J. A. Rogers, M. Hatalis, D. Temple, G. Moddel, *Proc. IEEE* **93**, 1239 (2005).
 - ¹³L. Gatzoulis and I. Iakovidis, *IEEE Eng. Med. Biol. Mag* **26**, 51 (2007).
 - ¹⁴J.-H. So, J. Thelen, A. Qusba, G. J. Hayes, G. Lazzi, and M. D. Dickey, *Adv. Funct. Mater* **19**, 3632 (2009).
 - ¹⁵S. Cheng, A. Rydberg, K. Hjort, and Z. Wang, *Appl. Phys. Lett* **94**, 144103 (2009).
 - ¹⁶R. C. Chiechi, E. A. Weiss, M. D. Dickey, and G. M. Whitesides, *Angew. Chem., Int. Ed* **47**, 142 (2008).
 - ¹⁷M. D. Dickey, R. C. Chiechi, R. J. Larsen, E. A. Weiss, D. A. Weitz, and G. M. Whitesides, *Adv. Funct. Mater* **18**, 1097 (2008).
 - ¹⁸T. Sekitani, Y. Noguchi, K. Hata, T. Fukushima, T. Aida, and T. Someya, *Science* **321**, 1468 (2008).
 - ¹⁹C. Kim, Z. Wang, H.-J. Choi, Y.-G. Ha, A. Facchetti, and T. J. Marks, *J. Am. Chem. Soc* **130**, 6867 (2008).
 - ²⁰A. C. Siegel, S. T. Phillips, M. D. Dickey, N. Lu, Z. Suo, and G. M. Whitesides, *Adv. Funct. Mater* **20**, 28 (2010).
 - ²¹L. Gatzoulis and I. Iakovidis, *IEEE Eng. Med. Biol. Mag* **26**, 51 (2007).
 - ²²B. A. Cetiner, H. Jafarkhani, J.-Y. Qian, H. J. Yoo, A. Grau, and F. De Flaviis, *IEEE Commun. Mag* **42**, 62 (2004).
 - ²³C.-P. Lin, C.-H. Chang, Y. T. Cheng, and C. F. Joo, *IEEE Antennas Wireless Propag. Lett* **10**, 1108 (2011).
 - ²⁴H.-J. Kim, C. Son, and B. Ziaie, *Appl. Phys. Lett* **92**, 011904 (2008).
 - ²⁵D.-H. Kim, J.-H. Ahn, W.-M. Choi, H.-S. Kim, T.-H. Kim, J. Song, Y. Y. Huang, L. Zhuangjian, L. Chun, and J. A. Rogers, *Science* **320**, 507 (2008).
 - ²⁶D.-H. Kim, J. Z. Song, W. M. Choi, H. S. Kim, R. H. Kim, Z. J. Liu, Y. Y. Huang, K. C. Hwang, Y. W. Zhang, and J. A. Rogers, *Proc. Natl. Acad. Sci. U.S.A.* **105**, 18675 (2008).
 - ²⁷O. Smiljanic, F. Larouche, X. L. Sun, J. P. Dodelet, and B. L. Stansfeld, *J. Nanosci. Nanotechnol* **4**, 1005 (2004).
 - ²⁸B. Aõssa, L. L. Laberge, M. A. Habib, T. A. Denidni, D. Therriault, and M. A. El Khakani, *J. Appl. Phys* **109**, 084313 (2011).
 - ²⁹B. Aõssa, E. Hafeez, N. Tabet, M. Nedil, D. Therriault, and F. Rogier, *Appl. Phys. Lett* **101**, 043121 (2012).
 - ³⁰L. L. Lebel, B. Aõssa, M. A. El Khakani, and D. Therriault, *Adv. Mater* **22**, 592 (2010).
 - ³¹B. Aõssa, E. Haddad, W. Jamroz, S. Hassani, R. D. Farahani, P. G. Merle, and D. Therriault, *Smart Mater. Struct* **21**, 105028 (2012).
 - ³²D. Therriault, S. R. White, and J. A. Lewis, *Nature Mater* **2**, 265 (2003).
 - ³³An Epon 828 based epoxy and SWNT nanocomposite filament of about 100 μ m in thickness was first deposited onto the PDMS substrate and serve as structural walls to contain the metal fluidic alloy nanocomposite.
 - ³⁴C.-S. Zhang, Q.-Q. Ni, S.-Y. Fu, and K. Kurashiki, *Compos. Sci. Technol.* **67**, 2973 (2007).